

Unified Approach to Synthesis of Mutators Employing Operational Transimpedance Amplifiers for Memristor Emulation

VIERA BIOLKOVÁ¹⁾, DALIBOR BIOLEK^{2,3)}, ZDENĚK KOLKA¹⁾
 Depts. of Radioelectronics ¹⁾ and Microelectronics ²⁾, Brno University of Technology
 Dept. of EE ³⁾, University of Defence Brno
 CZECH REPUBLIC
 dalibor.biolek@unob.cz <http://user.unob.cz/biolek>

Abstract: - A procedure of the synthesis of mutators for transforming the resistor with non-linear current-voltage characteristic into the memristor with equivalent-shape charge-flux constitutive relation is described. The final aim of the synthesis is the mutator implementation via operational transimpedance amplifiers. It will enable simple manufacture of analogue memristor emulators from off-the-shelf integrated circuits.

Key-Words: - Memristor, mutator, non-linear resistor, constitutive relation, synthesis, operational transimpedance amplifier.

1 Introduction

The fabrication of a memristive system, frequently denoted by the terms “TiO₂ memristor“ or “HP memristor“, in the Hewlett-Packard laboratories in 2008 [1], initiated an intense increase in the interest in this device, which was theoretically postulated in 1971 by L. Chua [2] as the fourth fundamental passive element. Since the TiO₂ memristor is still not available as a commercial component, the theoretical research proceeds with the support of computer models [3-8] or emulators [9-12]. The very first memristor emulation was described in the original paper [2], in which the memristor was introduced into the circuit theory. It is shown in [2] that the memristor can be emulated via mutators which can transform non-linear classical R, C, and L elements into memristors. Experiments with the so-called M-R mutator are subsequently described. This mutator transforms a resistor with non-linear current-voltage characteristic into a memristor with a similar shape of the charge-flux constitutive relation. The theory of the Type-1 and Type-2 mutators from [13] is used here. In [2], four basic variants of M-R mutator are introduced (Types 1 and 2, each of them being of Realizations 1 and 2), which are modeled via controlled sources. However, the concrete circuit implementation in [2] is rather complicated, which correlates with the level of the IC industry in the 1970s. In [14], the models of M-R mutators from [2] are generalized by introducing physical coefficients k_x and k_y . It is also shown here that the emulation of the passive memristor via the passive resistor can be done by means of 8 various mutator topologies. One of them is used in [14] for

the demonstration of a possible circuit implementation of the mutator via two transimpedance operational amplifiers (TOA), one classical voltage-feedback operational amplifier, two resistors, and two capacitors.

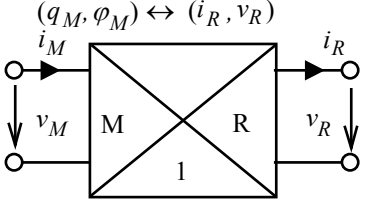
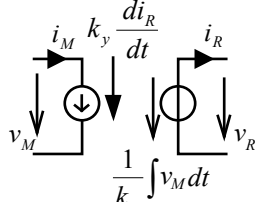
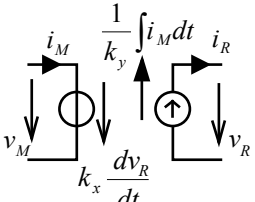
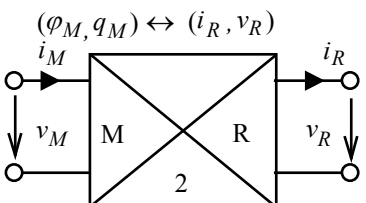
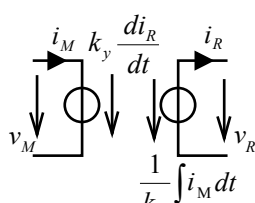
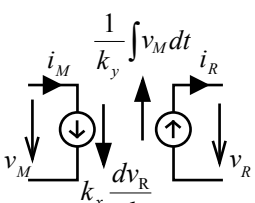
The present paper follows up on the works [2] and [14] and describes novel M-R mutators which were designed with regard to the following objectives: They must contain only one type of active components – TOA, which is commonly available on the market; the number of the active components must be as low as possible (by reason of simple circuitry and minimum power dissipation); it should contain only grounded passive R and C elements (in virtue of minimizing the influence of parasitic impedances and an easy on-chip implementation).

The paper has the following structure: The basic facts about M-R mutators and their behavioral models from [2] and [14] are summarized first. The next Section explains the methodology of mutator synthesis from the above models with the help of TOAs. Novel circuit topologies of mutators designed via this methodology are given in Section 4. One of them is selected for verification, both via PSpice simulation and via measurements on mutator specimens.

2 M-R mutators

Consider the cases of voltage- or current-controlled resistors with $i_R(v_R)$ or $v_R(i_R)$ characteristics, which represent unambiguous functions of voltage v_R or current i_R . It is necessary

Table 1: Two types and four basic realizations of M-R mutator [14].

type	symbol	implementation using controlled sources	
		realization 1	realization 2
1			
2			

to transform these characteristics into the $q_M(\varphi_M)$ or $\varphi_M(q_M)$ characteristics of flux (φ)- or charge (q)-controlled memristors. The mutator in Table 1, denoted Type 1, transforms the voltage-controlled resistor into flux-controlled memristor or the current-controlled resistor into charge-controlled memristor according to the linear transformation

$$\varphi_M = k_x v_R, \quad q_M = k_y i_R \quad (1)$$

where k_x and k_y are real constants whose values depend on the mutator implementation.

Eqs. (1) can be rewritten in the form

$$v_R = \frac{1}{k_x} \int v_M dt, \quad i_M = k_y \frac{d}{dt} i_R \quad (2)$$

which leads to the behavioral model denoted “Type 1-Realization 1” in Table 1.

Another form of (1),

$$v_M = k_x \frac{d}{dt} v_R, \quad i_R = \frac{1}{k_y} \int i_M dt \quad (3)$$

describes the “Type 1-Realization 2” model.

The Type-2 mutator provides other transformations, namely voltage-controlled resistor into charge-controlled memristor, and current-controlled resistor into flux-controlled memristor, according to the rules

$$q_M = k_x v_R, \quad \varphi_M = k_y i_R \quad (4)$$

The above procedure leads to two remaining behavioral models of “Type 2” in Table 1.

For Type-1 mutator, the memristance R_M of the emulated memristor depends on the differential

resistance R of the non-linear resistor as follows (see Eq. 1):

$$R_M = \frac{d\varphi_M}{dq_M} = \frac{k_x}{k_y} \frac{dv_R}{di_R} = \frac{k_x}{k_y} R. \quad (5)$$

Accordingly, the memductance G_M of the memristor emulated via Type-2 mutator is

$$G_M = \frac{dq_M}{d\varphi_M} = \frac{k_x}{k_y} \frac{dv_R}{di_R} = \frac{k_x}{k_y} R. \quad (6)$$

To emulate passive memristors from passive resistors, i.e. for $R > 0$ and thus $R_M > 0$, the physical constants k_x and k_y must be of the same signs, or

$$k_x k_y > 0. \quad (7)$$

In other words, both constants can be either positive or negative. As a result, two versions of potential circuit implementation lie behind each realization in Table 1, which differ in the orientations of the corresponding port quantities. From these eight possibilities, such should be selected that lead to an easy implementation based on TOAs, bearing in mind the goals of the synthesis specified in Section 1.

3 Methodology of mutator synthesis

The procedure of mutator synthesis with the use of TOAs will be explained on the example of the mutator of Type 1 Realization 1.

The basic block-oriented schematic of the TOA is shown in Fig. 1. The output current of the input voltage buffer is copied by a current mirror, and

thus it is also available at i terminal. The voltage of this terminal can be copied to low-impedance output v . The following important facts that can be used for the synthesis of the mutators from Table 1 appear from the following:

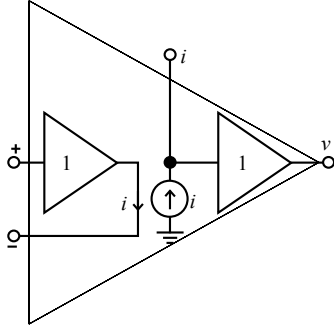


Fig. 1: Block diagram of the transimpedance operational amplifier (TOA).

1) The input buffer can be utilized as a controlled voltage source in Type-1 mutators and in Realization 1 of Type-2 mutator. The output current of this mutator is available at i terminal. It can be used for controlling other sources contained in the mutators.

2) The voltage-controlled current source can be implemented by connecting grounded impedance to the - terminal. Then + will be the controlling and i the output terminal. For the resistive or capacitive character of this impedance, the source current will depend on the control voltage or on its time-domain derivative.

3) From the point of view of the v terminal, TOA behaves as a voltage source controlled by current i , which flows through the output of the buffer after loading the i terminal by a grounded impedance. For the resistive or capacitive character of this impedance, the source voltage will depend on the control current i or on its time-domain integral.

4) The voltage-controlled voltage source and current-controlled current source can be implemented via cascading the sources from Items 2) and 3). In addition, the TOA contains two voltage-controlled voltage sources and one current-controlled current source with unitary gains.

5) The sign of the gain of the controlled current source can be modified via connecting the - terminals of two TOAs through a working impedance which is commonly grounded, or via connecting the i and - terminals of two TOAs.

Eight M-R mutators, which have the parameters of the four mutators from Table 1, are designed with the help of the above rules.

4 Novel M-R mutators

It follows from Table 1 that to implement the resistive port of the Type 1 Realization 1 mutator, it is necessary to sense the voltage of the memristive port, provide its time-domain integration, and then control by this quantity the voltage source connected to the resistive port. Then it is necessary to sense the current flowing through the resistive port and control the current through the memristive port via the time-domain derivative of the sensed current.

A possible solution is indicated in Fig. 2 (a). The voltage v_M is brought to the resistor R_i by amplifier No. ①. The current of this resistor is conveyed to the capacitor C_i . The capacitor voltage is then given by the integral of the voltage v_M divided by the time constant $R_i C_i$. The amplifier No. ② transmits this voltage to the resistive port. The corresponding physical coefficient k_x is then $k_x = R_i C_i$.

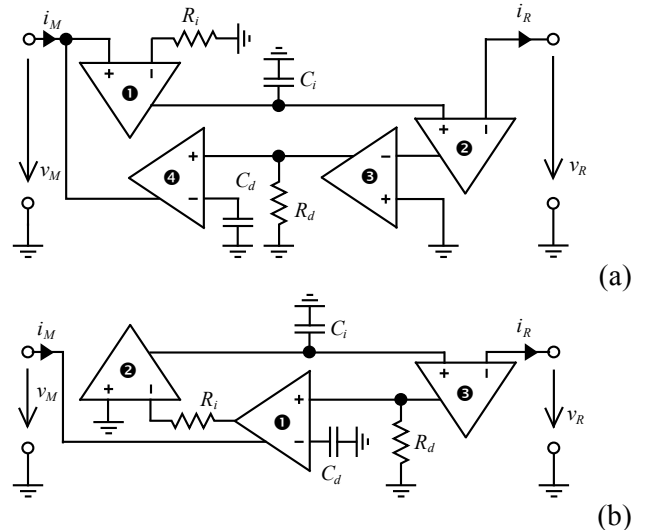


Fig. 2: Two versions of M-R mutator, type 1, Realization 1.

The current i_R of the resistive port is conveyed via amplifier No. ② to its current output which is connected to the inverting input of amplifier No. ③. The purpose of this amplifier with grounded non-inverting input is to invert the current, sensed from the resistive port, such that the resulting current which must supply the memristive port will be in the correct direction. This inverted current is transformed via R_d into a voltage, which is then transferred to the capacitor C_d by means of amplifier No. ④. The capacitor current is then given by the derivative of the current through the resistive port multiplied by the time constant $R_d C_d$. This current is then conveyed to the memristive port via the current output of amplifier No. ④. Note that the coefficient k_y is equal to the time constant $R_d C_d$. According to (5), the emulated memristance is

$$R_M = \frac{R_i C_i}{R_d C_d} R. \quad (8)$$

A certain drawback of this mutator can be seen in the necessity of utilizing four TOAs. A more economical version is given in Fig. 2 (b). The voltage of the memristive port is copied by the internal buffer of amplifier No. ❶ to the voltage output or to the resistor R_{i_s} , which is pseudo-grounded by the inverting input of amplifier No. ❷. A copy of the current of this resistor is conveyed to the capacitor C_i . Its voltage is copied by amplifier No. ❸ to the resistive port. In comparison with the schematic in Fig. 2 (a), the voltage is inverted, and the coefficient k_x changes its sign. To emulate the passive memristor, the other coefficient k_y must be also negative. This can be accomplished by the same method as for the circuit in Fig. 2 (a) but omitting the “current inversion” and thus saving one amplifier. This economical circuitry in Fig. 2 (b) is then modeled by the same relation (8) between the memristance and the resistance as for the circuit in Fig. 2 (a).

A similar procedure can be applied to other mutators in Table 1.

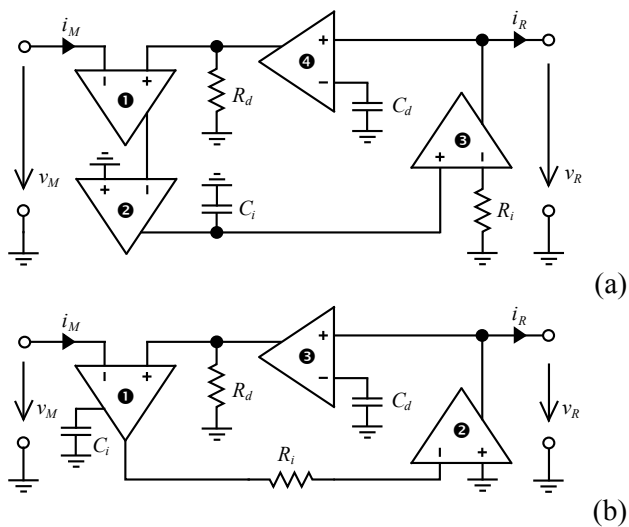


Fig. 3: Two versions of M-R mutator, type 1, Realization 2.

Two versions of Type 1, Realization 2 mutator are shown in Fig. 3. Amplifiers No ❶, ❷, and ❸ in Fig. 3 (a) together with C_i and R_i transfer the current i_M into current i_R which is the integral of the current i_M with the respective time constant $R_i C_i$. Then amplifiers No. ❹ and ❶ together with C_d and R_d serve as a derivative converter of voltage v_R to current i_M with the time constant $R_d C_d$. The economical version in Fig. 3 (b) omits one amplifier since it also uses the voltage output of amplifier No.

❶ to excite the resistor R_{i_s} , which is grounded in the original circuitry. This trick changes the direction of the current through this resistor. Both circuits are thus characterized by positive coefficients k_x and k_y and by relationship (8) between the resistance and the memristance.

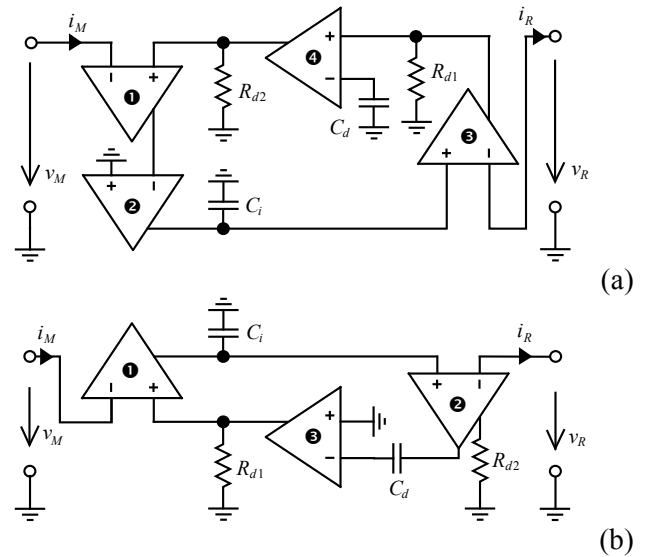


Fig. 4: Two versions of M-R mutator, type 2, Realization 1.

Figure 4 (a) shows a Type 2 Realization 1 mutator with four TOAs. Amplifier No. ❸ behaves at the resistive port as a voltage source which is controlled by the integral of the current i_M . This integration is done via floating the current through the capacitor C_i , thus $k_x = C_i$. Amplifier No. ❶ behaves at the memristive port as a voltage source, its voltage being given by the derivative of the current i_R , whereas $k_y = R_{d1} R_{d2} C_d$. The resistance-memductance relationship is (see Eq. (6))

$$G_M = \frac{C_i}{R_{d1} R_{d2} C_d} R. \quad (9)$$

The circuit in Fig. 4 (a) is rather complicated. On the other hand, it has only grounded passive elements.

The circuit in Fig. 4 (b) employs only three TOAs but the signals are transmitted between the gates as inverted in comparison with the previous mutator. The coefficients k_x and k_y are thus negative. Eq. (9) holds true also for this circuit.

Fig. 5 demonstrates two Type 2 Realization 2 mutators. Note from Table 1 that these mutators work as voltage sources controlled by the integral or derivative of the corresponding gate voltages. The circuit (a) is characterized by the coefficients $k_x = C_d$, $k_y = R_{i1} R_{i2} C_i$. These coefficients are negative for the circuit (b). Eq. (6) is now

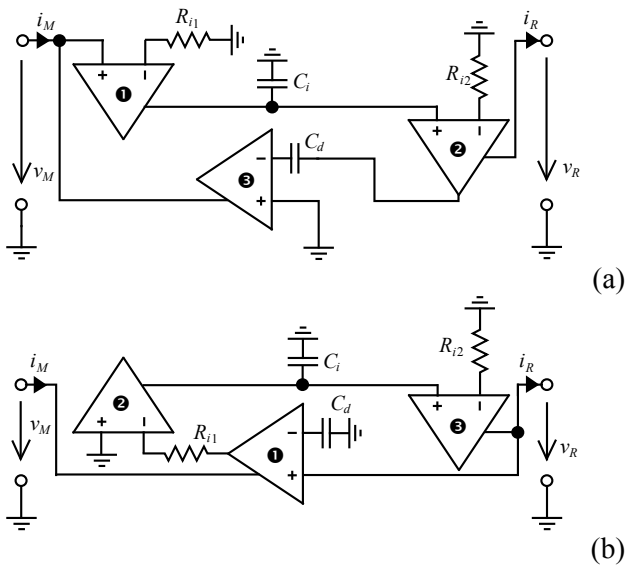


Fig. 5: Two versions of M-R mutator, type 2, Realization 2.

$$G_M = \frac{C_d}{R_{d1} R_{d2} C_i} R. \quad (10)$$

5 Experimental verification

The designed mutators were implemented in two ways, by means of AD844 commercial amplifiers, and with the help of low-voltage low-power TOAs described in [15]. The non-linear resistive load for all mutators was built identically as in [14] via a LED circuit shown in Fig. 6.

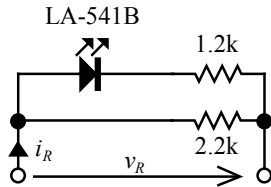


Fig. 6: Implementation of non-linear load of M-R mutators [14].

In the first step, all the mutators were simulated, utilizing the SPICE models of the active components, under the excitation of periodical signals. It was proved that the emulated memristors exhibited all the typical fingerprints, i.e. identical zero-level crossing points of voltage and current waveforms, pinched hysteretic loops in the current-voltage characteristics, fading of the hysteretic effects with growing frequency, and the independence of the memristor charge-flux constitutive relation from the method of memristor excitation.

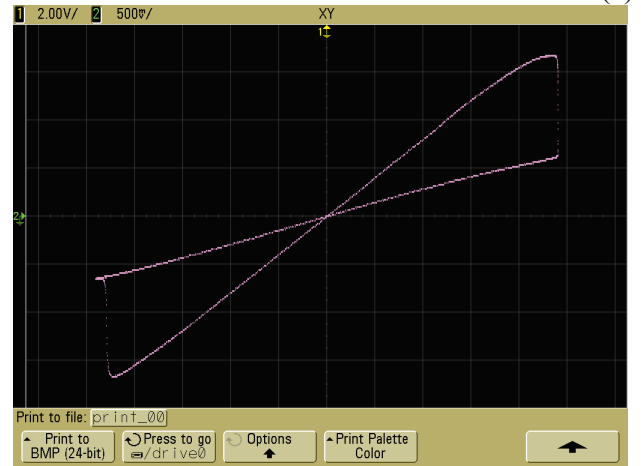
In the second step, the above experiments were repeated with the manufactured prototypes of

selected mutators. Figure 7 shows measured waveforms for the Type 1 Realization 1 mutator from Fig. 2 (b). The mutator was fabricated on the basis of three AD844 TOAs with symmetrical power supplies of $\pm 15\text{V}$ and with the parameters $R_i = 5\text{ k}\Omega$, $R_d = 1\text{ k}\Omega$, $C_i = C_d = 300\text{ nF}$.

Both capacitors were shunted by $50\text{ k}\Omega$ resistors in order to eliminate the offset voltage [14]. The mutator was excited from the functional generator by a $10\text{ V}/100\text{ Hz}$ harmonic voltage. The measured waveforms of port voltage $v_M(t)$ and current $i_M(t)$ and the pinched hysteretic loop, typical of a memristor, are shown in Fig. 7.



(a)



(b)

Fig. 7: (a) Measured voltage (upper curve) and current waveforms of memristor emulated via mutator in Fig. 2 (b), (b) pinched hysteretic loop.

6 Conclusion

The methodology of the synthesis of mutators for transforming nonlinear resistors into memristors with the help of transimpedance operational amplifiers is described. It is shown that these amplifiers enable an easy implementation of voltage

and current sources which can be controlled by time-domain integrals and derivatives of other voltage and current signals in the circuit. Starting from this methodology, it is possible to generate a set of various topologies of the mutators. One can select a circuit that best complies with the designer requirements. The functionality of the designed mutators has been verified both via computer simulation and also through measurements on manufactured prototypes.

Acknowledgments

This work has been supported by the Czech Science Foundation under grant No P102/10/1614, by the project CZ.1.07/2.3.00/20.0007 WICOMT of the operational program Education for competitiveness, and Project for the development of K217 Department, UD Brno – Modern electrical elements and systems.

References:

- [1] Strukov, D.B., Snider, G. S., Stewart, D. R., and Williams, R. S. The missing memristor found. *Nature*, vol. 453, 2008, pp. 80–83.
- [2] Chua, L. O. Memristor – The missing circuit element. *IEEE Trans. Circuit Theory*, vol. CT-18, no. 5, 1971, pp. 507–519.
- [3] Biolek, Z., Biolek, D., and Biolková, V. SPICE model of memristor with nonlinear dopant drift. *Radioengineering*, vol. 18, no. 2, 2009, pp. 210–214.
- [4] Benderli, S., and Wey, T.A. On SPICE macromodelling of TiO₂ memristors. *Electronics Letters*, vol. 45, no. 7, 2009, pp. 377–379.
- [5] Shin, S., Kim, K., and Kang, S-M. Compact models for memristors based on charge-flux constitutive relationships. *IEEE Trans. Computer-Aided Design of Int. Circ. Syst.*, vol. 29, no. 4, 2010, pp. 590–598.
- [6] Biolek, D., Biolek, Z., and Biolková, V. SPICE modeling of memristive, memcapacitative and meminductive systems. In *Proc. European Conf. on Circuits Theory and Design*, Antalya, Turkey, 2009, pp. 249–252.
- [7] Prodromakis, T., Boon, P. P., Papavassiliou, C., and Toumazou, C. A versatile memristor model with nonlinear dopant kinetics. *IEEE Trans. Electron Devices*, vol. 58, no. 9, 2011, pp. 3099–3105.
- [8] Biolkova, V., Kolka, Z., Biolek, Z., Biolek, D. Memristor modeling based on its constitutive relation. In *Proceedings of the European Conference of Circuits Technology and Devices (ECCTD'10)*, Puerto De La Cruz, Tenerife, Spain, 2010, pp. 261-264.
- [9] Valsa, J., Biolek, D., and Biolek, Z. An analogue model of the memristor. *Int. J. Numer. Modelling. Electronic Networks, Devices and Fields*, vol. 24, no. 4, 2011, pp. 400–408.
- [10] Sodhi, A., Gandhi, G. Circuit mimicking TiO₂ memristor: A plug and play kit to understand the fourth passive element. *International Journal of Bifurcation and Chaos*, vol. 20, no. 8, 2010, pp. 2537–2545.
- [11] Pershin, Y. V., and Di Ventra, M. Practical approach to programmable analog circuits with memristors. *IEEE Trans. Circuits Syst. I, Reg. Papers*, vol. 57, no. 8, 2010, pp. 1857–1864.
- [12] Kolka, Z., Biolek, D., and Biolková, V. Hybrid modelling and emulation of mem-systems. *Int. J. Numer. Modelling. Electronic Networks, Devices and Fields*, published online 8 Aug 2011.
- [13] Chua, L. O. Synthesis of new nonlinear network elements. *Proceedings of the IEEE*, vol. 56, no. 8, 1968, pp. 1325–1342.
- [14] Biolek, D., Bajer, J., Biolková, V., Kolka, Z. Mutators for transforming nonlinear resistor into memristor. In *Proc. European Conf. on Circuits Theory and Design*, Linköping, Sweden, 2011, pp. 509-512.
- [15] Biolek, D., Biolková, V., Kolka, Z. Low-Voltage-Low-Power Current Conveyor for Battery Supplied Memristor Emulator. In *5th International Conference on Circuits, Systems and Signals (CSS'11)*, Corfu, Greece, 2011, pp. 171-175.